CHEMCOMM
Feature Article
www.rsc.org/chemcomm

Unique acid catalysis of heteropoly compounds (heteropolyoxometalates) in the solid state

Makoto Misono

Department of Environmental Chemical Engineering, Kogakuin University, 1-24-2 Nishi-Shinjuku, Shinjuku-ku, Tokyo 163 8677, Japan. E-mail: misono@cc.kogakuin.ac.jp

Received (in Cambridge, UK) 20th March 2001, Accepted 11th May 2001
First published as an Advance Article on the web

Fundamental and superior characteristics of heteropoly compounds (heteropolyoxometalates) in the solid state that make them suitable for catalyst design at the atomic/molecular levels are described, together with important principles required for the understanding and design of solid heteropoly catalysts. First, the molecular nature of heteropolyanions (metal oxide clusters), which can be preserved in the solid state, enables control of the acid and redox properties over a wide range. Second, the presence of hierarchical structures (primary, secondary and tertiary structures) can lead to three catalysis modes—surface-type, pseudoliquid (or bulk-type I) and bulk-type II. Precise control of pore size is possible through the understanding of the microstructure, which results in unique shape selectivity observed for various reactions. Heteropoly compounds are green catalysts functioning in a variety of reaction fields and efficient bifunctional catalysts when combined with other components. The elucidation of catalytic processes is also possible at the atomic/molecular level due to their molecular nature. The positions and dynamic nature of protons as well as organic reaction intermediates in the pseudoliquid phase can be clarified by spectroscopic techniques. Various reactions promoted by solid heteropoly catalysts are collected from recent publications to illustrate the usefulness of the above ideas and of heteropoly catalysts themselves.

1 Catalyst design at the atomic/molecular level

1.1 Importance and feasibility

Efficient catalysts are key materials in chemical technologies which supply useful substances to society and assist maintaining the environment as healthy as possible: in short, catalysts represent a key technology for a sustainable society. Although recent progress has been remarkable for homogeneous and biochemical catalysts, in particular the latter, heterogeneous (solid) catalysts are still of substantial importance in catalytic technology, and have several advantages. Therefore development of these is centred to solving global and local problems.

It is much more difficult to design heterogeneous catalysts than to interpret reactions over model solid catalysts. Hence, the development of practical (or commercial) catalysts still mostly relies on trial-and-error approaches, assisted by phenomenological knowledge on existing commercial catalysts and sophisticated knowledge on simple model catalysts. The design of practical catalysts at the atomic or molecular level has long been pursued,[1,2] since precisely designed multifunctional catalysts are obviously desirable. However, catalyst design at this level is still a distant goal in many instances.

1.2 Our approach

We have endeavored in the last two decades to establish the methodology of catalyst design by studying crystalline mixed oxides. In addition to their crystallinity, our criteria to choose catalyst materials are; (i) wide variation of composition whilst retaining the basic crystal structure and (ii) catalytic performance near the level required for practical application. Such materials include heteropoly compounds, perovskite-type mixed oxides and zeolites whose structures can be well defined at least for the solid bulk phases. Differences between the surface and solid bulk phase appear to be much smaller for these metal oxides than for metallic catalysts. This is particularly true for heteropoly compounds if the preparation and characterization of catalysts are carefully carried out. Here, the term 'heteropoly compounds' (abbreviated as HPAs) will be used for heteropolyoxometalates which include heteropolyacids and their derivatives. Heteropolyacids are hydrogen forms of heteropolyanions produced by the condensation of more than two kinds of oxoanions. Typical heteropolyanions are shown in Fig. 1. Using heteropoly compounds we attempted to establish the following relationships at the atomic/molecular levels as shown in Scheme 1.

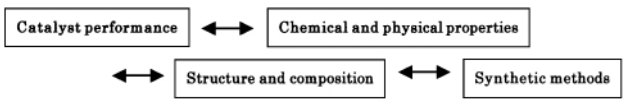

Scheme 1

This article reports important progress to establish the basis for catalysts design since the publication of special issue of *Chemical Reviews* on polyoxometalates in 1998.[3] It will attempt to show that heteropoly compounds have various attractive and important characteristics in terms of catalysis and are promising materials for catalyst design at the atomic/molecular level.

Makoto Misono received his Bachelor, Master, and Doctor's degree in Engineering from the University of Tokyo and started his academic career in 1966 at the University of Tokyo, where he became a full professor in 1983. He spent two years in the USA for his postdoctorate (1967–1969; at the University of California, Santa Barbara, and Mellon Institute, Pittsburgh). He has been studying heterogeneous catalysis mainly of mixed oxides for 40 years and gave a plenary lecture at the 10th International Congress on Catalysis, Budapest, in 1992 on the subject of molecular catalyst design of solid heteropoly compounds. Since his retirement from the University of Tokyo with the Emeritus professorship in 1999, he has been a professor at Kogakuin University, a private technical university located in the center of Tokyo. He is a former president of Catalysis Society and a vice president of Chemical Society of Japan. He was elected a member of Science Council of Japan in 2000. He is now more involved in various activities related to the environment and chemistry such as green/sustainable chemistry and clean fuel-exhaust of automobiles.

DOI: 10.1039/b102573m

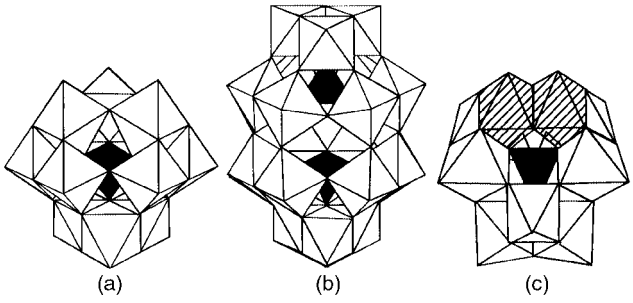

Fig. 1 Examples of heteropolyanions: (a) Keggin-type polyanion *e.g.* α-$PW_{12}O_{40}^{3-}$, (b) Dawson-type polyanion *e.g.* $P_2W_{18}O_{62}^{6-}$; (c) disubstituted polyanion *e.g.* γ-$SiW_{10}Fe_2O_{40}^{10-}$.

Catalysts based on heteropoly compounds are hereafter denoted heteropoly (or HPA) catalysts. Earlier books and review articles may be referred to regarding the basic chemistry[4] and general catalysis[5] of HPAs. HPA catalysts have already been applied to several large-scale commercial processes.[6]

2 Basic concepts unique for solid HPA catalysts

In my view, the following concepts are essential to understand and design HPA catalysts, in addition to the knowledge generally required to understand heterogeneous catalysis of the ordinary mixed oxides.

2.1 Primary, secondary and tertiary structures

At an early stage of our study it was recognized that the hierarchical structure of solid HPAs was important for the understanding of the heterogeneous HPA catalysis, and we denoted the substructures as primary, secondary and tertiary.[7] This may appear a very simple idea, but enormously helped the progress of our research. Fig. 2 shows a simplified illustration of such hierarchical structures. The primary structure is the structure of heteropolyanion itself *i.e.* the metal oxide cluster molecule and details the molecular nature of solid HPA catalyst. Fig. 2 shows the most ubiquitous form which has the Keggin structure. The secondary structure is the three-dimensional (usually regular) arrangement consisting of polyanions, counter cations and additional molecules. The secondary structure is flexible to different extents depending on the counter cation and the structure of the polyanion, and is the basis of bulk-type catalysis of solid HPA catalysts (see below). The tertiary structure represents the manner in which the secondary structure assembles into solid particles and relates to properties such as particle size, surface area, and pore structure,[8] and plays an important role in heterogeneous catalysis. Without understanding this hierarchical structure, one can neither understand solid HPA catalysts properly nor take advantage of their molecular nature, and the idea of bulk-type catalysis described below would not have evolved.

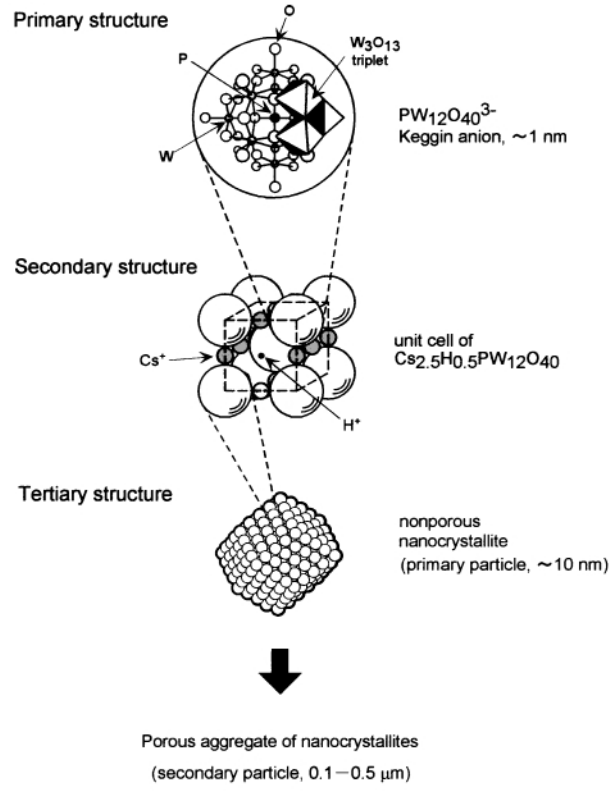

Fig. 2 Primary, secondary and tertiary structures; hierarchical structure of heteropoly compounds (HPAs) in the solid state.

2.2 Three types of catalysis

We have demonstrated that there are three totally different modes of catalysis for solid HPAs (Fig. 3). Surface-type catalysis (a) is ordinary heterogeneous catalysis which takes place on the solid surface (two-dimensional reaction field on outer surface and pore wall). Modes (b) and (c) represent bulk-type catalysis where the reaction fields are three-dimensional in contrast to the surface-type catalysis. When the diffusion of reactant molecules in the solid (diffusion in the lattice rather than pores) is faster than the reaction, the solid bulk forms a pseudo-liquid phase in which catalytic reaction can proceed [Fig. 3(b)]. In this instance, reactant molecules in the gas or liquid phase penetrate in between the polyanions (primary structure), sometimes expanding the distance between the polyanions, and react inside the bulk solid. The products come out to the surface and are released to the gas or liquid phase. Pseudoliquid catalysis, proposed in 1979, was not favourably accepted initially, since it appeared very unusual for heterogeneous mixed oxide catalysts. Now, however, such catalysis is more firmly established.[5a–c] In the pseudoliquid phase such catalysts appear as solids but behave like liquids (solvent). As the active sites in the solid bulk *e.g.* protons, take part in catalysis, very high catalytic activities are often observed in the bulk phase. Phase transitions accompanied by an abrupt change in catalytic performance are also observed.[5a]

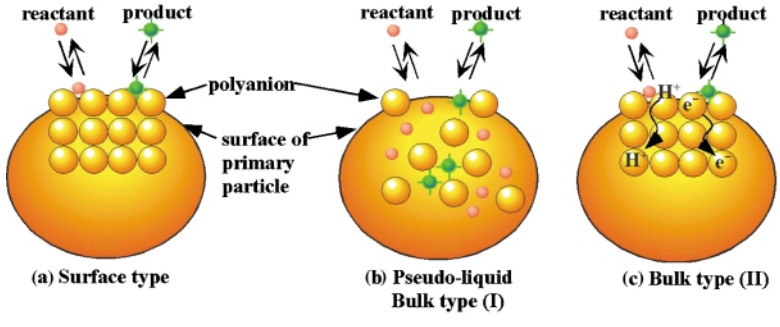

Fig. 3 Three types of catalysis for solid heteropoly compounds: (a) surface type; (b) pseudoliquid: bulk type (I), (c) bulk type (II).

The second bulk-type catalysis [bulk-type (II), Fig. 3(c)] is found for oxidation catalysis at high temperature when the diffusion of redox carriers (protons and electrons in this case) is rapid in the solid bulk, and the whole bulk participates in the reduction–oxidation cycle.[9] It should be noted that, as the contribution towards catalysis of the solid bulk varies with the relative rate of diffusion to that of reaction, intermediate cases between surface and bulk catalysis arise. Solid HPAs containing cations of low ionic radii to charge ratio (H^+, Na^+, Cu^{2+}, *etc.*) readily absorb small polar molecules and tend to exhibit pseudoliquid behaviour and are soluble in water. Cs and NH_4 salts (scarcely soluble in water, due to low solvation energy) usually show only surface-type catalysis.

The importance of this idea may be clearly understood by the following examples. Fig. 4(a) plots the relative activity and number of strong acid sites *vs.* the extent of neutralization (or the Na content) for acidic Na salts of $H_3PW_{12}O_{40}$.[10] Hereafter, $H_3PW_{12}O_{40}$, one of the most widely used HPA catalysts is abbreviated as HPW unless stated otherwise. The reactions are of bulk type (I) and the acidity is related to the number of protons in the entire bulk. It is evident in Fig. 4(a) that the rates of bulk-type reactions and the bulk acidity decrease monotonically with the Na content, thus showing good parallelism between catalytic activity and acidity. This also demonstrates that the acid catalysts can be designed by control of their acidity in this manner. In contrast, no monotonical change is found for several reactions catalyzed by acidic Cs salts, $Cs_xH_{3-x}PW_{12}O_{40}$ (denoted CsX), as shown in Fig. 4(b).[5a,b,11] These reactions are of surface type, as revealed by plots of the rates *vs.* the *surface acidity* (number of protons on the surface). The surface area sharply rises from 1–2 $m^2\ g^{-1}$ for Cs1 and Cs2 to *ca.* 150 $m^2\ g^{-1}$ for Cs3. The mechanism of the increase in surface area is interpreted in a later section of the article. As is obvious in Fig. 4(c), a good correlation is obtained.[12] Another important point to be noted is that the specific activity of CsX [catalytic activity per surface proton, the slope in Fig. 4(c)] is much higher than known solid acids such as zeolites and silica–alumina. This fact demonstrates the high performance of HPA catalysts.

Bulk-type catalysis (II) is also an essential concept required to understand and design HPA catalysts.[13] This has been found to be relevant for oxidation reactions at high temperatures. If the rates of *bulk-type oxidation* (*e.g.* oxidative dehydrogenation) are plotted against the surface redox property, very poor correlations are found, but the rates exhibit good correlations with *bulk* redox property. In contrast, the rate of *surface-type* oxidation correlates very well with the *surface redox property*. This is very similar to the acid catalysis shown in Fig. 4. Without knowing this fact, the development of practical oxidation catalysts would be very difficult.

2.3 Merits of HPA catalysts

The advantages of hetreopoly compounds for heterogeneous catalysts are summarized in Table 1.[5] There are several large-scale industrial processes utilizing HPA catalysts as oxidation and acid catalysts both in the solid state and in solution.[5a,b,6] Most are environmentally friendly, so that HPA catalysts are regarded as promising green (or sustainable) catalysts.[14,15]

Table 1 Merits of solid heteropoly catalysts for catalyst design at the atomic/molecular level

1	Systematic variation of acid and redox properties are possible for catalyst design.
2	Molecular nature of solid heteropoly compounds originating from heteropolyanion molecules enables precise design of catalysts and molecular description of catalytic processes
3	A variety of reaction fields are available for catalytic systems.
4	The unique basicity of polyanions

3 Novel aspects of pseudoliquid catalysis

3.1 Variety of reaction fields

Pseudoliquid behavior [bulk-type (I) catalysis] has also been found for liquid–solid heterogeneous systems. For example, the relative catalytic activities of HPW and Cs2.5 dramatically change with the polarity of reacting molecules;[5b] HPW > Cs2.5 for pinacol rearrangement (pseudoliquid catalysis) and HPW < < Cs2.5 for alkylation of aromatics (surface-type catalysis). HPW shows high activities for the reactions in the solid bulk (pseudoliquid), since protons inside the solid can be utilized, while Cs2.5 having a large quantity of protons on the surface (see below) is active for surface-type reactions. Bulk type (II) catalysis has not yet been observed probably because the reaction temperatures are low. The various reaction fields containing a liquid phase are illustrated in Fig. 5.

The catalysis of solid HPAs in the liquid phase has been well documented.[16] For example, three reactions differing in polarity of reactants were compared using several alkali- and alkaline-earth salts of HPW. It was shown that the decomposition of cyclohexyl acetate is catalyzed on the solid surface (surface-type), and that pinacol rearrangement proceeds in the pseudo-liquid phase. On the other hand, esterification of benzoic acid and butan-1-ol is mainly catalyzed by HPA dissolved in solution, although most of HPA remains in the solid state. The order of catalytic activity, therefore, is very different between the reactions. This again demonstrates the importance of distinguishing surface- and bulk-type catalysis for the catalyst

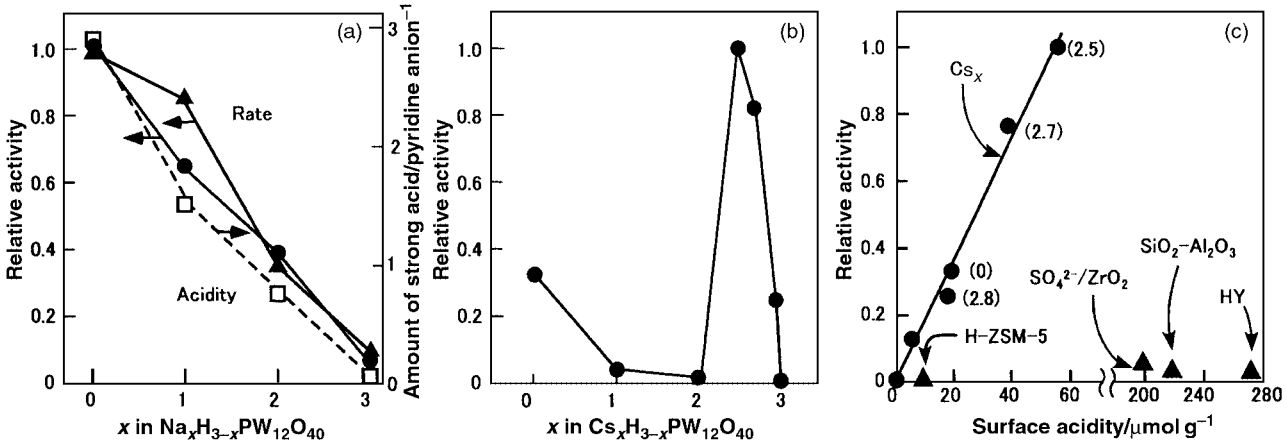

Fig. 4 Importance of differentiating surface- and bulk-type catalysis. (a) Bulk-type (I) (pseudoliquid) catalysis and bulk acidity of Na salts of $H_3PW_{12}O_{40}$ (HPW): (▲) conversion of methanol, (●) dehydration of propan-2-ol, and (□) bulk acidity measured by strongly held pyridine. (b) Rates of alkylation of 1,3,5-trimethylbenzene by cyclohexene catalyzed by Cs salts of HPW (surface-type catalysis). (c) Rates of alkylation over Cs salts [data from Fig. 4(b)] are plotted *vs.* the surface acidity, together with the same plots for several other solid acids.

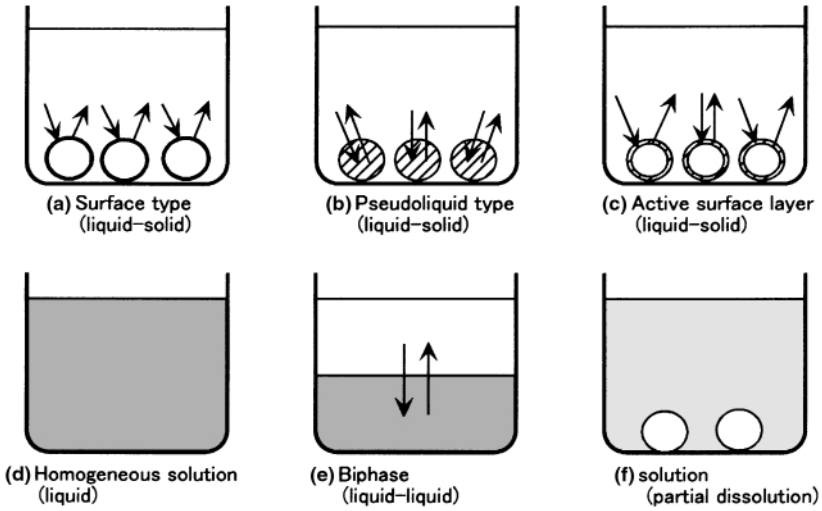

Fig. 5 Various reaction fields of HPA catalysis in reaction systems containing a liquid phase.

design of HPAs. Fig. 5(a) and (d) correspond to the ordinary heterogeneous catalysis (liquid–solid) and homogeneous (solution) catalysis, respectively. Phase-transfer catalysis for liquid–liquid biphase systems [Fig. 5(e)] is well known and there are at least two large-scale commercial processes using HPA catalysts.[6,14] Catalysis by solid HPAs for solid state reactions[17] and in a new phase formed on the surface layer[14] [Fig. 5(c)] are new. In the latter, protons introduced on the surface layer of Cs3 create a new active phase similar to a 'pseudoliquid' (Fig. 6).

Among other recent interesting observations is the unique relationship between the shape of the primary structure, the resulting secondary structures, and the remarkable influence on the catalytic activity.[18] The thermodynamically favored synthesis of methyl *tert*-butyl ether (MTBE) from isobutylene and methanol proceeds at low temperature (323 K) on Dawson-type hetropolyacids ($H_6P_2W_{18}O_{62}$ and $H_6P_2Mo_{18}O_{62}$) rapidly and selectively. In contrast, the reaction is very slow over Keggin-type heteropolyacids, in spite of the higher acid strength and comparable acid content. We found that Dawson-type heteropolyacids are amorphous under the reaction conditions due to the ellipsidal shape of the polyanion, whereas Keggin-type polyanions having spherical shape are crystalline (bcc structure). Owing to this difference the former forms active pseudoliquids, while the latter are much less active (Table 2). As for MTBE synthesis catalyzed by $H_4SiW_{12}O_{40}$, Bielanski's group has made an extensive study and proposed a hypothesis that the reaction takes place on the surface to which methanol and protons are supplied from the pseudoliquid phase.[19]

3.2 Protons, water and organic molecules in pseudoliquids

To understand and design pseudoliquid catalysts at the molecular level, information about the acidic protons, such as their location, mobility and donating ability (acid strength), is indispensable. Information about the interactions between acidic protons and small basic molecules such as water and alcohols provides useful knowledge about pseudoliquid catalysis, since water is often contained in the working state and plays an important role. Furthermore, the states and dynamics of protons in the solid are interesting subjects of solid-state chemistry. In our early studies we observed protons in HPW using MAS NMR, then directly detected (by a combination of NMR and IR) the reaction intermediates of ethanol dehydration in the pseudoliquid phase, and disclosed the dynamic behavior of methanol.[5b,6]

While IR is usually a powerful tool to study solid catalysts the IR spectra of OH bands of heteropolyacids are ambiguous. For highly hydrated HPW, the OH stretching and bending modes of water and protonated water are detectable, but for more dehydrated states they do not show any clear IR bands in contrast to silica or zeolite catalysts.

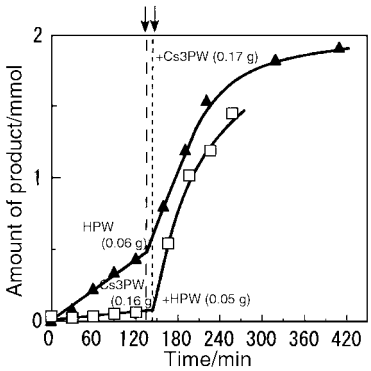

Fig. 6 Catalysis in a novel phase formed on the surface layer of a solid HPA for a liquid–solid reaction system. Hydrolysis of bistrimethylol propane monoformal in water at 348 K. The reaction rate rises sharply when the second component is added after a certain reaction time (indicated by arrows). The rates after the addition are much higher than the sum of the rates of each component, indicating the formation of an active layer on the surface of Cs3.

Table 2 Unique relationships between shape of polyanion (primary structure), secondary structure and catalytic activity

Primary structure[a] (shape)	Secondary structure at the working state	Catalytic activity for MTBE synthesis at 323 K
Dawson (ellipse) $H_6P_2W_{18}O_{62}$ $H_6P_2Mo_{18}O_{62}$	Amorphous	Very high
Keggin (spherical) $H_3PW_{12}O_{40}$ $H_4SiW_{12}O_{40}$	Crystalline (bcc)	Very low

[a] See Fig. 1.

Recently, reliable IR spectra of HPW·$n$$H_2O$ with different degrees of hydration have been reported independently by us[20b] and Zecchina's group.[21] Fig. 7 shows our results where the water contents are quantified (reliable at least for n = 0 and 6). Very broad bands ranging from 3500 to 1200 cm^{-1} are evident. For n = 6 (hexahydrate) for which the structure has been established,[5] an extremely broad band is observed which we assigned to $H_5O_2^+$ ($H_2O\cdots H^+\cdots OH_2$) present in the hexahydrate. A broad band having a peak at about 3200 cm^{-1} was observed for dehydrated sample (n = 0–0.5), which was

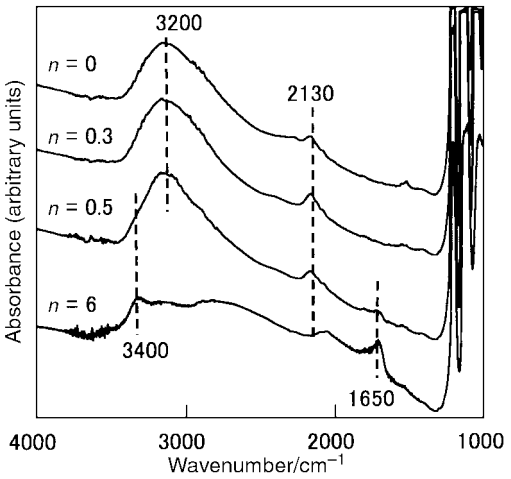

Fig. 7 IR spectra of $H_3PW_{12}O_{40}{\cdot}nH_2O$ with a variety of hydration states ($0 < n < 6$).

assigned to isolated acidic protons bonded to peripheral oxygens of the polyanion. These bands seem to exist in the IR spectra reported in earlier studies, but their presence and significance have not been well recognized.

Zecchina's group reported high quality IR spectra and provided valuable discussion of the IR bands.[21] The extremely broad band observed for the hexahydrate is reasonably interpreted by the nearly flat potential of a proton in a hydrogen bond. However, they possibly underestimated the water content of some samples (see below) and therefore their assignment of the IR bands is probably partially incorrect. The evacuation of hydrated HPW at 300–340 K leads to the hexahydrate which is fairly stable.[5a–c] Usually a higher temperature (as high as *ca.* 350 K) is necessary for further dehydration. Therefore, the sample of Zecchina's group which was obtained upon evacuation at room temperature for 3 min has probably $n > 6$, whereas the sample obtained by evacuation for 150 min is most likely the hexahydrate.

The states and dynamics of protons and water in HPW have been clarified by an extensive study using solid-state ^1H, ^{31}P and ^{17}O MAS NMR.[22] For example, the P NMR spectra of $HPW{\cdot}nH_2O$ (n = 0–6) which was prepared from the hexahydrate by evacuation at 373–423 K are shown in Fig. 8. H NMR spectra measured at 298 and 173 K showed a very broad peak for $n = 6$ due to the dipole–dipole interaction in $H_5O_2^+$, and a sharp peak for the other samples. The following important conclusions can be deduced from the NMR data.

(a) Acidic protons are present in three forms; (i) proton attached to polyanions, (ii) H_3O^+ (hydronium ion monomer) or H_2O strongly interacting with acidic protons, and (iii) $H_5O_2^+$ (hydronium ion dimer). H_3O^+ and $H_5O_2^+$ weakly interact with polyanions by hydrogen bonding. Acidic protons in the anhydrous sample attach to the polyanion leading to a significant chemical shift in the ^{31}P NMR spectrum. The probable bonding states are schematically illustrated in Fig. 9.

On the basis of IR studies, Zecchina's group concluded that for intermediate hydration states ($0 < n < 3$), the acidic proton does not form H_3O^+ but rather O–H···OH_2 .[21] However, the close resemblance in the chemical shifts of the P NMR spectra (*e.g.* $n = 2.1$ measured at 173 K, Fig. 8) and of CsX[8,25] suggests the formation of H_3O^+; acidic protons interact very weakly with polyanions. The remainder of the acidic protons remain directly bonded to the polyanions. It should also be noted that the acid strength of HPW is greater than that of zeolites (see below, Table 3).

(b) The broad peak observed at 298 K (n = 0 .5–4) splits into several peaks at 173 K (Fig. 8, $n = 0.5$, 2.1 and 4.0). This means that the rate of proton migration (exchange) is slow at 173 K and at 298 K is of the order of 200 Hz which is much faster than the rate of ordinary catalytic reactions. This study also indicated

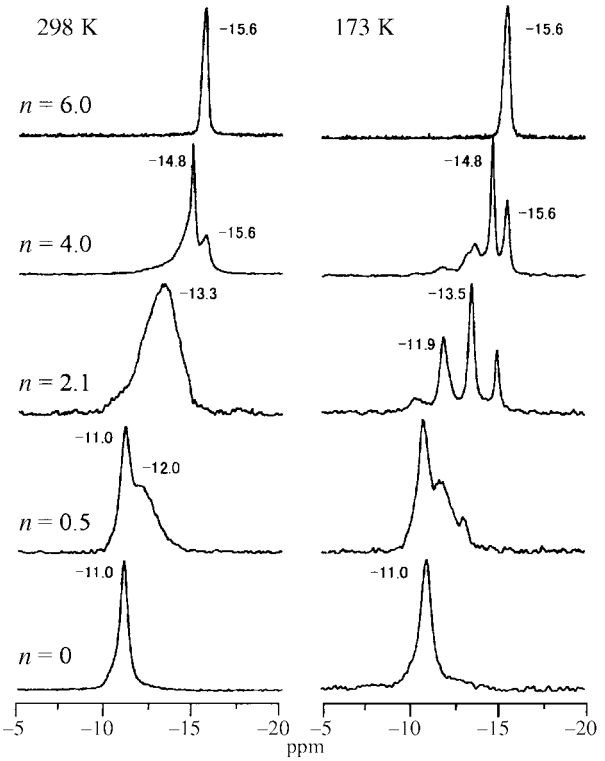

Fig. 8 ^{31}P NMR spectra of $H_3PW_{12}O_{40}{\cdot}nH_2O$ with a variety of hydration states ($0 < n < 6$) measured at 298 and 173 K.

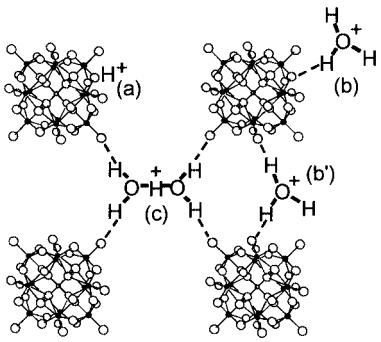

Fig. 9 Models proposed for the states of acidic protons and water in solid $H_3PW_{12}O_{40}{\cdot}nH_2O$ ($0 < n < 6$); two possible positions are shown for H_3O^+.

Table 3 Acid strengths of various solid acids

Solid acid	Initial heat of NH_3 sorption/kJ mol^{-1}	Approximate peak temperature of NH_3 desorption/K
$H_3PW_{12}O_{40}$	195	850
$Cs_{0.5}H_{2.5}PW_{12}O_{40}$	170	830
SO_4/ZrO_2	165 (190)[a]	1000 (as N_2)
HZSM-5 (Si/Al = 13)	150	670
SiO_2-Al_2O_3	145	600

[a] Value in parentheses refers to the very initial value.

that water in the lattice enhances the mobility of protons. The high mobility of protons may facilitate protonation in acid catalysis.

(c) The relative intensities of the split peaks follow a binominal distribution, indicating a uniform (random) distribution of protons and water in the solid.

(d) In the anhydrous state ($n = 0$), there is one type of acidic proton species attached to the polyanion at least on the NMR time scale. This is consistent with our IR data. We observed an apparently single broad band for the dehydrated sample (n = 0).

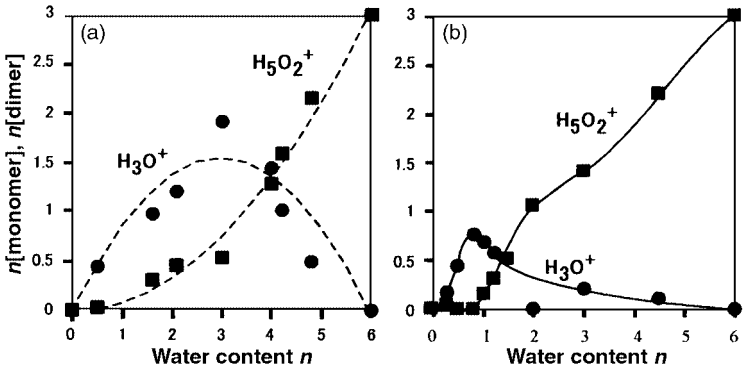

Fig. 10 Amounts of H_3O^+ (monomer) and $H_5O_2^+$ (dimer) per polyanion in $H_3PW_{12}O_{40}{\cdot}nH_2O$ ($0 < n < 6$). (a) Samples prepared by evacuation of the hexahydrate at 373–423 K. Dashed lines were calculated by assuming that water molecules are randomly removed from the hexahydrate. (b) Samples prepared by rehydration of anhydrous $H_3PW_{12}O_{40}$ at room temperature.

(e) The concentrations of the three proton species in $HPW{\cdot}nH_2O$ (n = 0–6) change with the extent of dehydration as shown in Fig. 10(a). The trends are in agreement with those calculated by assuming random removal of water.

In contrast, $HPW{\cdot}nH_2O$ prepared by the addition of water to an anhydrous sample at room temperature is quite different [Fig. 10(b)]. The main reason for the difference may be the lower temperature of preparation for which the diffusion of water is slow. Rehydration leads mainly to $H_5O_2^+$ instead of H_3O^+ at $n > 2$. Careful preparations are always necessary to obtain HPA samples having uniform composition. In particular, special caution must be taken to avoid rehydration, since anhydrous HPAs are very sensitive to moisture (even from water adsorbed on walls of apparatus).

3.3 Acidity

The acid strength of HPAs vary in a wide range depending on the polyanion structure and its constitutuent elements (both hetero and addenda atoms), as well as on the extent of hydration and reduction. Most results indicate that HPW after dehydration, the strongest HPA known so far, is a much stronger solid acid than zeolites including ZSM-5, and is close to that of superacids.[5,23] Indeed some believe HPW to be a superacid[24] while others claim that its acidity is comparable with zeolites.[21] The counter cation is also an important factor. Table 3 summarizes the acid strength as monitored by ammonia sorption (adsorption and absorption) and desorption for several solid acids,[23,25] and Fig. 11 shows the results of calorimetric measurements of NH_3 sorption on Cs2.5 and HPW at 423 K. Caution in interpretation of the results may be necessary for HPW which tends to exhibit pseudoliquid behaviour. Ammonia is absorbed into the bulk and forms ammonium salts, so that the lattice energy of the salts should be considered in calculating the heat of sorption.

Quantum chemical studies with higher levels of approximation on a full Keggin unit have recently been attempted. The stronger acidity of HPW than $H_3PMo_{12}O_{40}$ (HPMo) is indicated by density functional theory (DFT).[26] In early calculations, the position of protonation was inferred to be at bridging oxygen atoms.[27] Recently the same conclusion was deduced by a DFT calculation applied to a full Keggin unit including geometrical optimization.[28] Our ^{17}O MAS NMR and IR data are in agreement with this conclusion.[20b,22]

There are at least five different mechanisms for the evolution of acidity of solid HPA salts[5a] and hence the acidic properties are complicated unless the structures are carefully scrutinized. NMR studies revealed that protons of a novel nature are formed by the reduction of Ag and Pd salts of HPW.[29] Protons are reversibly formed by the reduction of $Ag_3PW_{12}O_{40}$ and are much more catalytically active than the protons in HPW for several reactions in the presence of H_2. ^1H NMR spectroscopy showed that protons in the former are more mobile than those of the latter. The influence of the mobility of protons on catalytic performance is an interesting topic. Similar behaviour is observed for Ag zeolites and can be formulated by reactions (1)–(3).[29c]

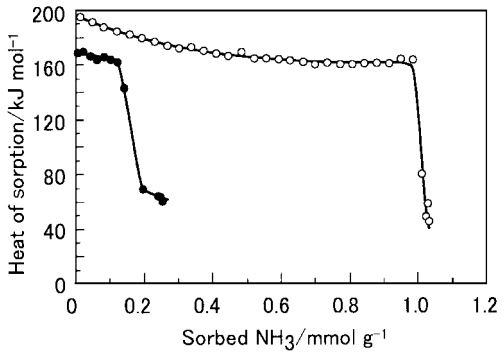

Fig. 11 Differential heats of NH_3 sorption measured at 423 K: (○) $H_3PW_{12}O_{40}$, (●) $Cs_{2.5}H_{0.5}PW_{12}O_{40}$.

$$2Ag^+ + H_2 \rightarrow 2Ag^0 + 2H^+ \quad (1)$$

$$2Ag^0 + Ag^+ \rightarrow Ag_3^+ \quad (2)$$

$$Ag_3^+ + H_2 \rightarrow Ag_3H + H^+ \quad (3)$$

4 Recent topics in surface-catalysis of Cs and NH_4 salts of HPW

4.1 Microstructure

The microstructure, or the tertiary structure (particle size, surface area, pore distribution, *etc.*) of insoluble acidic Cs and NH_4 salts of HPW is of great interest since Cs2.5 showed extremely high catalytic activities for various reactions in the liquid phase as a strong solid acid.[5a–c] The activity is often more than ten times greater than that of zeolites and more than three times that of the parent HPW. Activity much higher than that of HPW was also reported for Cs2.4 prepared in a slightly different manner.[30] Furthermore, the size of the micropores of Cs2.5 is nearly uniform, can be controlled at the sub nm level and leads to remarkable shape selective catalysis.[23,31] Acidic NH_4 salts are also active and for benzoylation $(NH_4)_4HPW_{12}O_{40}$ was more acive than Cs2.5.[32] Ag and Tl salts seem to have similar microstructures.[33]

The main reason for the high activity of Cs2.5 is its high surface acidity *i.e.* the large number of strongly acidic protons on the surface.[5a–c] The number of surface sites is about half of the total number of protons contained in the solid owing to its high surface area (*ca.* 150 $m^2\ g^{-1}$). Cs2.5 is a strong acid being only slightly weaker than the parent HPW (Table 3). Other

reasons for the high activity are moderate hydrophobicity of the surface, a bimodal pore distribution and acid–base bifunctionality (see below). All of these factors are interesting and important for heterogeneous catalysis.

Extensive and detailed studies using ^{31}P NMR, XRD, electron diffraction, AFM and SEM, adsorption of N_2, Ar, *etc*, as well as quantitative chemical analysis, have recently been carried out to clarify the microstructures of the acidic Cs and NH_4 salts.[25] Those measurements were applied comprehensively to the preparation processes *i.e.* solutions, precipitates and resulting solids obtained after drying and heat treatment, and provided a consistent view about the microstructures of Cs2.5 and other CsX salts. Their formation processes thus deduced are schematically illustrated in Fig. 12.

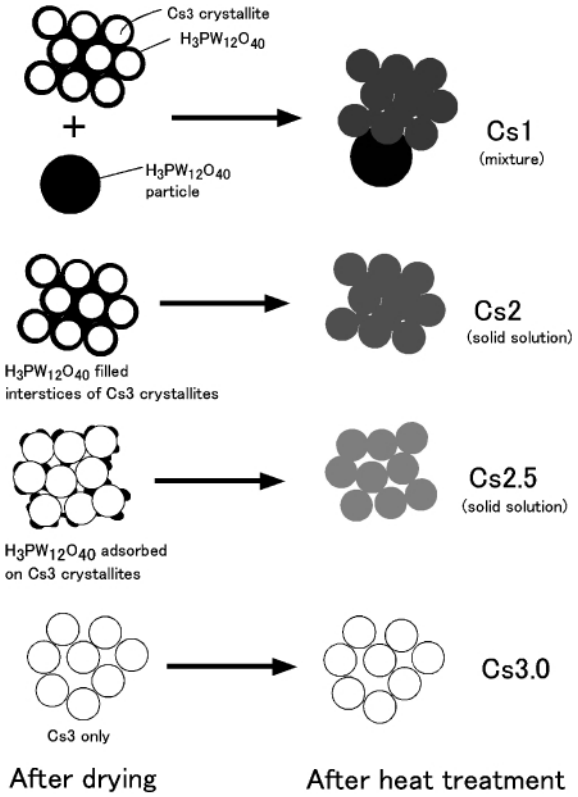

Fig. 12 Schematic illustration of the formation processes of acidic Cs salts: Left; after drying, right; after heat treatment.

Upon titration of an aqueous solution of HPW with a Cs_2CO_3 aqueous solution at 298 K, very fine precipitates of Cs3 (nanoparticles of *ca*. 10 nm in diameter) are formed, to which HPW is partly adsorbed with the remaining HPW present in the solution. As the titration proceeds, the amount of HPW in solution decreases, forming Cs3 precipitates. At the stoichiometry of Cs2 (Cs_2CO_3 added: HPW = 1 : 1), the precipitates are fine particles (also *ca*. 10 nm in diameter) of Cs3, the surface of which are covered by nearly a monolayer of HPW. Their surface area is very low (1 $m^2\,g^{-1}$), since the fine particles stick together densely after drying. This model is supported by the fact that the particle size estimated from XRD linewidths is *ca*. 10 nm, while that estimated from the BET surface area is 500 –1000 nm.

When Cs_2CO_3 is added beyond a stoichiometry of X = 2, the surface area increases sharply, since most of HPW precipitates as Cs3 and the amount of HPW remaining in solution or adsorbed on precipitates diminishes rapidly. Hence, micropores start to develop which would have been absent if the remaining HPW had densely connected the nanoparticles. ^{31}P NMR (which can differentiate between polyanions containing 0, 1, 2 or 3 protons) demonstrated that thermal treatment at 373–473 K leads to a nearly uniform solid solution of $Cs_3PW_{12}O_{40}$ (Cs3) and $H_3PW_{12}O_{40}$ (HPW) *via* diffusion of protons and Cs^+ ions, the lattice constant changing accordingly. This process has been unambiguously confirmed by the formation of the identical solid solutions when Cs3, impregnated by various amounts of HPW, is treated at 473 K, as shown by the P NMR spectroscopy (Fig. 13).

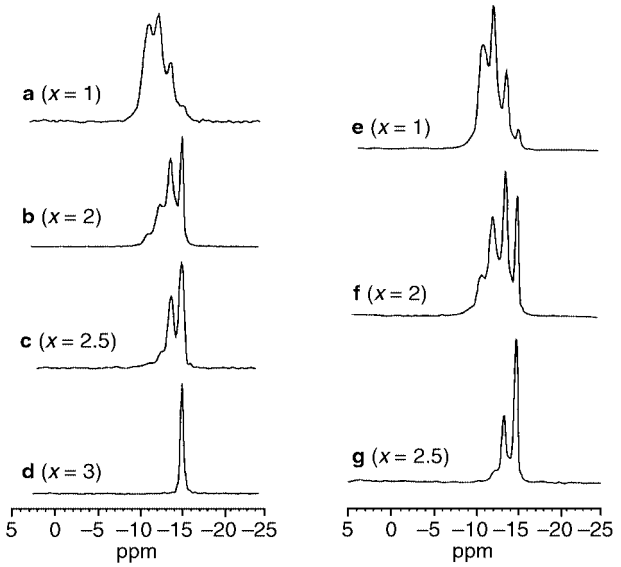

Fig. 13 Comparison of the ^{31}P NMR spectra of $Cs_xH_{3-x}PW_{12}O_{40}$ (CsX) [(a)–(d)] with Cs salts having the same compositions (CsX, X = 1, 2, 2.5) prepared by impregnation of $Cs_3PW_{12}O_{40}$ (Cs3) by HPW [(e)–(g)]. All samples were thermally treated at 473 K.

Cs2.5 has a bimodal pore size distribution; micropores ranging from 0.5 to 1.0 nm (peak at 0.65 nm and mostly > 0.75 nm) and mesopores (peak at 4–5 nm).[30,34] It is deduced that the micropores arise from spaces between nanocrystallites (10–20 nm) in loose and random aggregates and mesopores arise from spaces between the nanocrystallites and between aggregates of size *ca*. 100–500 nm (see Fig. 2). The micropores account for about 70% of the total surface area of Cs2.5 [see below, Fig. 15(d)]. Misfits in the connection of nanocrystallites have recently been suggested as the origin of small micropores (see below).[35] Another possible origin of micropores are polyanion vacancies as proposed for $Cs_4PMo_{11}VO_{40}$.[36] However, no firm and detailed conclusion has been obtained for the origin of the micropores which have a rather sharp size distribution.

A surprising finding of the microstructure is the epitaxial assembly of Cs and NH_4 salts, which was discovered unexpectedly [Fig. 14 and Fig. 15].[37,38] When the Cs salts are

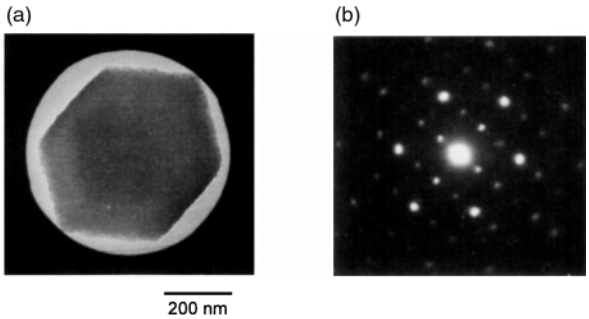

Fig. 14 Electron diffraction pattern of $(NH_4)_3PW_{12}O_{40}$ prepared by titration at 368 K using NH_4HCO_3: (a) the area in which the diffraction pattern was taken and (b) diffraction pattern.

prepared at a temperature as high as 370 K, the initially formed nanocrystallites (*ca*. 10 nm) assemble together with the identical orientation of crystal planes, leaving micropores between the nanoparticles [Fig. 15(b)], in contrast to Cs2.5

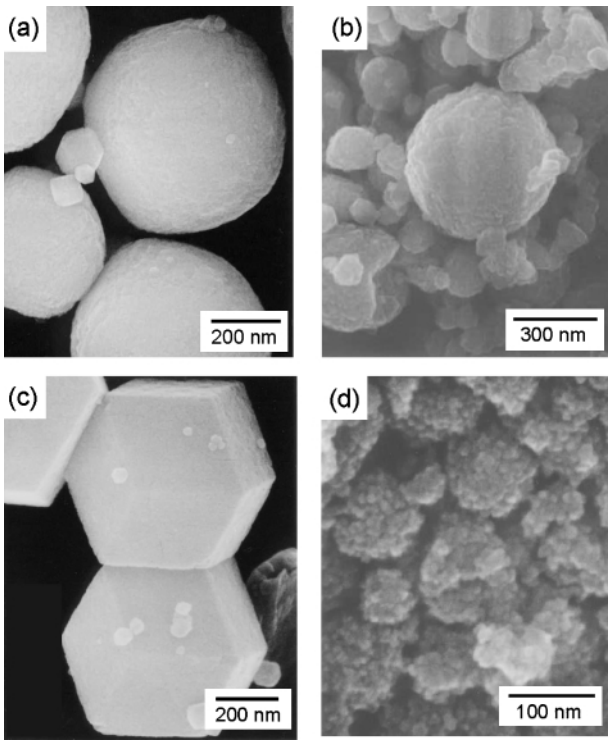

Fig. 15 SEM images of (a) $(NH_4)_3PW_{12}O_{40}$ prepared by titration at 273 K, (b) $Cs_3PW_{12}O_{40}$ (Cs3) prepared by titration at 368 K, (c) $(NH_4)_3PW_{12}O_{40}$ prepared by titration at 368 K and (d) $Cs_3PW_{12}O_{40}$ (Cs3) prepared by titration at 298 K. Cs2.5 is similar to Cs3 in appearance.

prepared at room temperature [Fig. 15(d)]. This is most remarkable when a stoichiometric NH_4 salt is prepared by means of homogeneous precipitation using urea decomposition.[34] The initially formed particles are spherical and slightly oriented aggregates [resembling the NH_4 salt formed by titration at low temperature shown in Fig. 15(a)], that are comprised of nanocrystallites of size *ca*. 10 nm with micropores (*ca*. 0.6 nm) in the spaces between the nanocrystallites, and mesopores (2–10 nm) between the loosely bound nanocrystallites and/or between the aggregates (100–1000 nm). The particles then gradually turn into large 'crystalline' microporous aggregates (400–1000 nm) having regular dodecahedral shape and few mesopores [similar to but larger than the particles shown in Fig. 15(c)]. The particle size estimated by XRD linewidth measurements (> 260 nm) is much greater than the size calculated from the surface area (10–20 nm), indicating that epitaxial connections occur between nanocrystallites. AFM and SEM images confirm that aggregates consist of fine particles of size *ca.* 10 nm. Electron diffraction (ED) shows regular discrete spots indicating crystallinity (Fig. 14). All of these observations indicate that the dodecahedral particles are 'crystalline' aggregates of nanoparticles and are porous. A monodispersed particle size (*ca*. 1000 nm) can be obtained by controlling the precipitation procedure (Fig. 16).[39] Spherical aggregates shown in Fig. 15(a) and (b) also give discrete ED patterns.

4.2 Shape selectivity

Remarkable shape selectivity has been reported for several acid-catalyzed reactions over Cs salts using molecules having different sizes. While Cs2.5 is active for most reactions, Cs2.1 and Cs2.2 only catalyzed reactions of small molecules.[5a,b,23] Shape selective catalysis has also recently been found for oxidation and hydrogenation reactions. Okuhara and coworkers confirmed that Cs2.1 has only micropores of size *ca.* 0.45 nm (in contrast to Cs2.5 for which both micropores of > 0.75 nm and mesopores of *ca*. 5 nm are present), and demonstrated shape selective catalysis, on the basis of the comparison of the catalytic activities of Pt-Cs2.1, Pt-Cs2.5 and Pt-SiO_2, for (i) oxidation of methane, carbon monoxide and benzene, and (ii) hydrogenation of ethylene and cyclohexene.[40] Shape selectivity in the products was found for the reaction of *n*-butane.[41] The large-pore Pt-Cs2.5 was very selective for the isomerization to isobutylene (94%), while cracked products (C_1–C_3) markedly increased with a decrease in the size of micropore (only 48% isobutene formed for Pt-Cs2.1) attributed to slow diffusion of the branched alkane in small micropores. Okuhara and coworkers proposed that small spaces formed by misfits in the connection of nanocrystallites are the origin of the small micropores of Cs2.1 (0.45 nm),[34] as illustrated in Fig. 17.

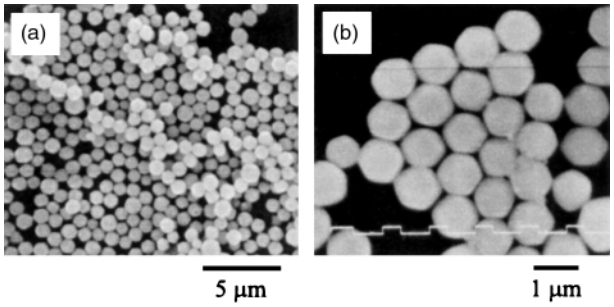

Fig. 16 SEM images of monodispersed $(NH_4)_3PW_{12}O_{40}$ prepared by titration at 368 K.

4.3 Surface acidity of $Cs_xH_{3-x}PW_{12}O_{40}$, CsX

The unusual change with X of the catalytic activity of CsX is reasonably interpreted by the surface acidity [Fig. 4(c)]. Here, the surface acidity is estimated by multiplying the number of polyanions on the surface (calculated from the surface area and the size of polyanion) and the number of protons per polyanion on the surface (from the proton content of the solid, or the chemical formula). Recently, the surface acidity, or the number of protons, on the surface of CsX (X = 2–3), has directly been measured by an IR study of CO adsorption at 110 K (Fig. 18).[20a] CO adsorbed on Cs2.5, for example, exhibits three bands; a band at 2165 cm^{-1} attributable to CO adsorbed on acidic proton sites, at 2154 cm^{-1} to CO on Cs^+ ion, and at 2139 cm^{-1} to physisorbed CO [Fig. 18(d)]. For comparison, the IR spectra of Cs3 is also shown, where both the 2165 cm^{-1} band and a broad band in the OH stretching region are absent [Fig. 18(b)].

As expected, the intensity of the first band (2165 cm^{-1}, CO on proton site) changed in parallel with the catalytic activity as shown in Fig. 19.[20a] In this way, the surface acidity estimated previously as described above has been confirmed by the direct measurement of the surface proton sites. None of the IR bands of adsorbed CO were detected for CsX (X = 0–2). Even if the very low surface areas of these Cs salts (X = 0–2) are taken into account, the IR bands would have been detected at least for HPW (4–5 $m^2\ g^{-1}$). The reason for the absence of the IR bands for HPW is not clear.

4.4 Hydrophobicity: water-tolerant solid acid catalysts

It has been shown in an earlier study that the surface of organic salts of HPW exhibit hydrophobicity.[42] Recently, the hydrophobicity was semi-quantitativley evaluated for Cs2.5 and Cs3 by comparison of water and benzene adsorption.[43] The hydrophobicity thus evaluated is in the order of HZSM-5 (high silica) > silica ≈ Cs3 > Cs2.5 ≈ HZSM-5 (low silica) > silica–alumina > alumina (ZSM-5 and silica were pretreated at 673 K, silica–alumina and alumina at 573 K, and Cs2.5 and C3 at 473 K). This indicates that Cs2.5 is moderately hydrophobic similarly to low-silica HZSM-5. As expected from this fact, it was demonstrated that Cs2.5 was very active as a water-tolerant solid acid catalyst.[44,45] The relative activity of water-tolerant solid acids varies with the nature of the reaction. Cs2.5 is usually much more active for the hydrolysis of esters than other inorganic solid acids, but less active than acidic organic resins.

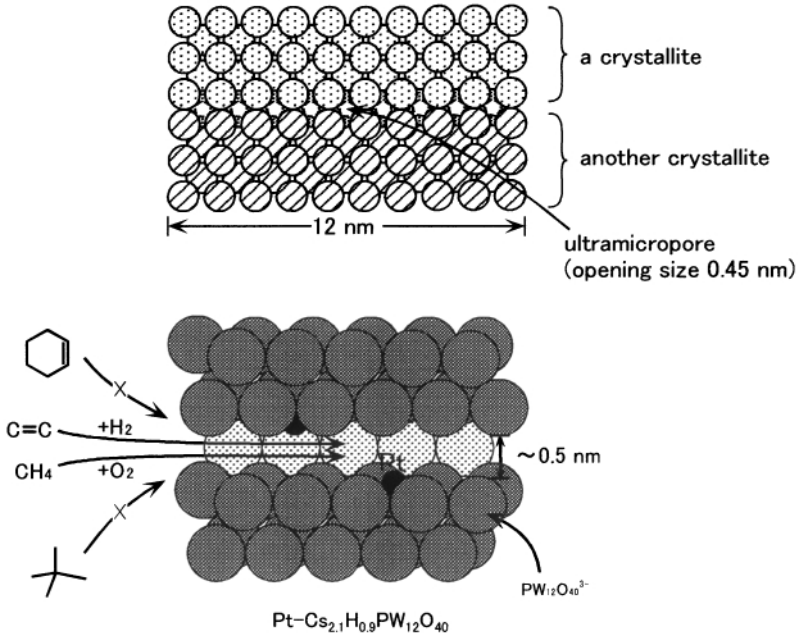

Fig. 17 A model of small micropores formed by misfits of two naoncrystallites of Pt–$Cs_{2.1}H_{0.9}PW_{12}O_{40}$.

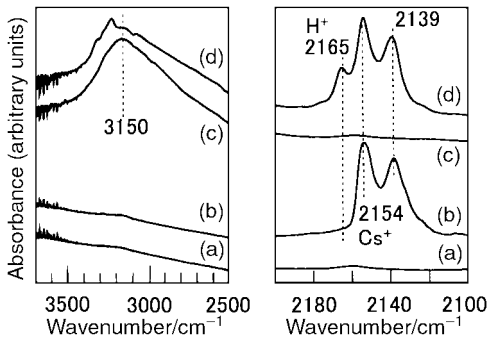

Fig. 18 IR spectra of CO adsorbed on HPAs measured at 100 K. (a) Before and (b) after adsorption of CO on $Cs_3PW_{12}O_{40}$ (Cs3); (c) before and (d) after adsorption of CO on $Cs_{2.5}H_{0.5}PW_{12}O_{40}$.

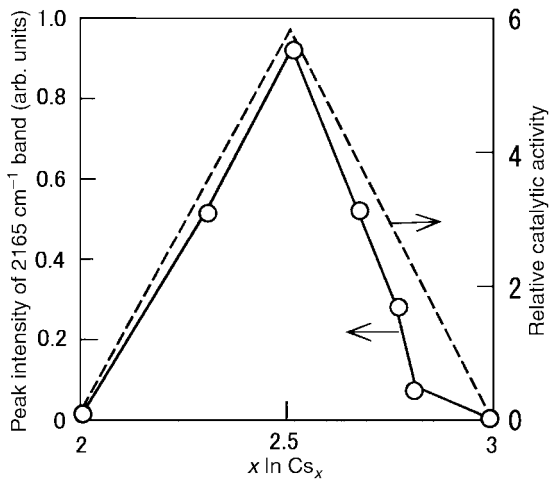

Fig. 19 Changes of the peak intensity of the 2165 cm^{-1} band (CO adsorbed on proton sites) and the catalytic activity of $Cs_xH_{3-x}PW_{12}O_{40}$ (CsX) as a function of X for the rate of alkylation of 1,3,5-trimethylbenzene by cyclohexene at 353 K.

However, for the reaction of a nitrile and an alcohol in an excess of water, Cs2.5 was the most active as shown in Table 4.[45]

5 Efficient catalysts developed based on HPA

Table 5 lists recent examples of catalytic reactions using solid HPA. Earlier examples may be found in ref. 5(*b*).

Table 4 Comparison of catalytic activities of various solid acids for the reaction of acrylnitrile and *N*-adamantanol to form *N*-adamantylacrylamide (NAA) in the presence of an excess of water.[a] Results in the absence of water shown in parentheses

Catalyst	Yield[b](%)	Selectivity[c](%)	TON[d]
$Cs_{2.5}H_{0.5}PW_{12}O_{40}$	84 (97)	92 (93)	36 (42)
HY zeolite	8 (79)	82 (89)	2 (0.2)
Amberlyst 15	68 (100)	82 (81)	1 (1)
Nafion-H	77 (97)	84 (92)	6 (8)
Nafion-SiO_2	40 (97)	94 (93)	22 (61)

[a] *Reaction conditions*; catalyst: 0.2 g, acrylnitrile: 60 mmol, 1-adamantanol: 1.3 mmol, 373 K, 6 h. [b] % Yield; 100 × (NAA formed)/(*N*-adamantanol added). [c] % Selectivity; 100 × (NAA formed)/(NAA formed + acrylamide formed). [d] TON (turnover number); mol NAA formed/mol acid sites in catalyst.

5.1 Bifunctional catalysts

HPAs show acidity as well as unique basicity; these properties as well as their oxidizing ability can be controlled over a wide range which is of use in catalyst design. The co-existence of these properties can be utilized to prepare bifunctional and multifunctional catalysts. It has been shown that the oxidation of methacrolein to methacrylic acid proceeds in two steps; the first step is acid-catalyzed esterification to form an intermediate and the second step the oxidation of the intermediate which is rate-determining. Hence this reaction can be catalyzed in a synergistic manner utilizing acidity and oxidizing ability.[7] It is interesting to note that these two properties compete in the case of oxidation of isobutyric acid to methacrylic acid, with acidity accelerating side-reactions (Scheme 2).

The much higher activity of Cs2.5 than conventional solid acids can not be explained by acidic properties alone [Fig. 3(c)], so that acid–base bifunctional catalysis was suggested for Cs2.5.[5b]

Efficient catalytic reactions can be realized by the combination of HPA catalysts with noble metals. One-stage oxidation of ethylene to acetic acid has been commercialized (10000 ton yr^{-1}) by combining a Keggin-type HPA catalyst and Pd.[46] Here, the addition of Se or Te to Pd is essential to suppress the complete oxidation to CO_2. The overall reaction [eqn. (6)] is suggested to proceed in two steps [eqn. (4) and (5)], a Wacker-type mechanism (*via* acetaldehyde) being excluded. Control of acidity and tertiary structure was important for catalyst

Table 5 Acid-catalyzed reactions with solid heteropoly compounds[a]

Reaction	Catalyst	Reference
$RCO_2H + R'OH \rightarrow RCO_2R'$	$H_3PW_{12}O_{40}$, $H_4SiW_{12}O_{40}$/MCM-41	59
Alkylation of alkylphenol by isobutylene (shape selective)	$H_3PW_{12}O_{40}$/MCM-41	53*b*
Trioxane + phenol	Silica-included $H_3PW_{12}O_{40}$	60
Isobutane + n-butenes $\rightarrow$ C_8 alkylates	$H_3PW_{12}O_{40}$/MCM-41	61
	$K_{2.6}H_{0.4}PW_{12}O_{40}$ (supercritical)	62
Diels–Alder reaction of quinone	$H_3PW_{12}O_{40}$	63
Acylation of xylene	$Cs_2HPW_{12}O_{40}$	53*a*
Adamantylamide synthesis	$Cs_{2.5}H_{0.5}PW_{12}O_{40}$	45
Hydration of dimethylbutene	$Cs_{2.5}H_{0.5}PW_{12}O_{40}$	44*a*
n-C_n $\rightarrow$ iso-C_n	$(NH_4,Cs,H)_3PW_{12}O_{40}$ Pt-$Cs_{2.5}H_{0.5}PW_{12}O_{40}$	64
Oxidation of ethylene to acetic acid *via* ethanol	Pd(Te)-$SiW_{12}O_{40}$ (commercialized)	46
Ethyl acetate from acetic acid	HPA (commercialized)	
Michael addition	$H_3PW_{12}O_{40}$ (pseudoliquid)	16*a*
$EtC(CH_2OH)_2CH_2OCH_2OCH_2C(CH_2OH)_2Et + H_2O \rightarrow 2EtC(CH_2OH)_2CH_2OH + HCHO$	$H_3PW_{12}O_{40}$, *etc*. (a new phase?)	14

[a] These reactions are mostly taken from a list produced by Professor T. Okuhara.

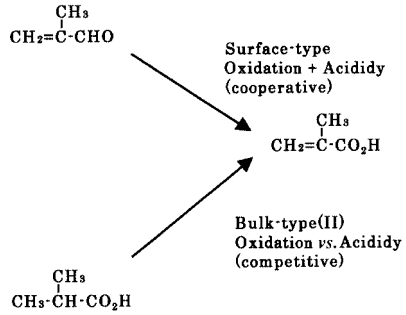

Scheme 2

development. (The photo on the cover is the plant used for this process developed by Showa Danko, Co., Ltd.)

$C_2H_4 + H_2O \rightarrow EtOH$ (acid catalysis) (4)

$EtOH + O_2 \rightarrow MeCO_2H + H_2O$ (oxidation) (5)

$C_2H_4 + O_2 \rightarrow MeCO_2H$ [overall reaction] (6)

The combination of Pd or Pt with Cs2.5 creates active and selective catalysts for the isomerization of *n*-alkanes (C_4–C_7).[47] Deactivation and cracking which are significantly observed over Cs2.5 alone are dramatically diminished by the addition of noble metals in the presence of H_2. Without acidity, the activity is very low. Interestingly, acidity completely prevents the hydrogenolysis of alkanes catalyzed by noble metals. A mechanism essentially based on a classical bifunctional catalysis has been proposed; acid catalyzed isomerization + dehydrogenation–hydrogenation. Recently, a mechanistic study using ^{13}C labeled *n*-butane[48] has revealed that the selective isomerization to isobutane over Pt dispersed on Cs2.5 mostly takes place by a monomolecular mechanism, while the reaction proceeds less selectively *via* a bimolecular mechanism in the case of Cs2.5 alone (Scheme 3). At higher reaction temperatures, the

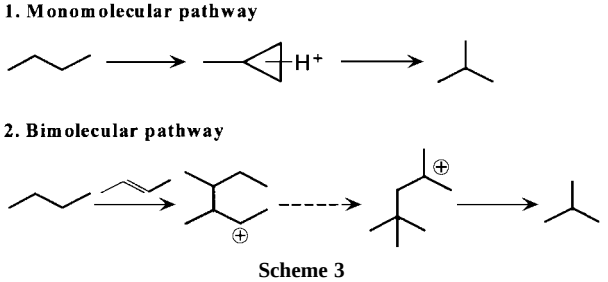

Scheme 3

contribution of the bimolecular mechanism increases also for Pt-Cs2.5. Kozhevnikov and coworkers reported that HPW combined with Pd produces only soft coke in the oligomerization of propene and the removal of coke by combustion takes place at a much lower temperature than in the case of HPW alone which forms both soft and hard cokes.[49]

5.2 Supported HPA catalysts

Hydrogen forms (or free acids) of HPAs usually have low surface areas. On the other hand, very active Cs2.5 having a large surface area tends to become a milky suspension during liquid-phase reactions, which makes it difficult to separate the catalyst after the reaction is finished. To solve these problems, many attempts have been made to disperse and fix HPA catalysts on various supports, where the stability of the HPA and firm fixation are the key issues. Support materials such as silica, carbon, and organic resins have been applied with varying levels of success, with new supporting materials and methods being actively pursued. Although the structure and composition of supported HPAs are sometimes uncertain, high catalytic activities are often observed and separation made easier.

Izumi *et al*, prepared HPW and Cs2.5 included in a silica matrix by an *in situ* sol–gel method. Recently, shape selectivity was observed for alkylation of phenol by formaldehyde owing to the micropores of a silica matrix.[50] Supported HPAs prepared by this method have been applied as photocatalysts.[51] Soled *et al*. reported an *in situ* preparation of Cs2.5 inside silica particles.[52] Cs-containing silica is added to an aqueous solution of HPA. As the HPA solution diffuses into pores of silica, a Cs salt starts to precipitate at a certain level of concentration, resulting in an egg-yolk type impregnation. Large-pore zeolites like MCM-41[53] and layered clays[54] have been applied as supports of HPA. HPAs loaded in layered double hydroxide were active for epoxidation and showed shape selectivity.[54] *In situ* synthesis of HPAs in the supercage of Y-zeolite is an interesting method for the preparation of supported HPA catalysts.[55] For metal oxide supports, interactions between the surface and the HPA often degrade the polyanion structure. On basic solids such as MgO and Al_2O_3, the Keggin structure readily decomposes, as expected from instability of HPAs in aqueous solution at high pH. Even on the surface of silica, which has only weak interactions with HPAs, these tend to decompose to smaller clusters. In most cases the decomposition is significant at a low loading level whereas the starting polyanion structure is predominant when the loading level is high. Supporting on or imbedding in organic polymers has also been attempted. Recent examples include polyazamethines,[56*a*] polyaniline,[56*b*] and polyphenylene oxide.[56*c*] As expected from

the moderate stabilities of organic ammonium and oxonium salts, the HPA structures appear to remain mostly intact. In addition, chemical interactions between the polymer and HPA sometimes modify the catalytic performance in a desirable manner.

6 Future

Notable progress has been achieved recently in heterogeneous acid catalytic reactions of HPAs. Full utilization of the pseudo-liquid phase and further development of bifunctional and shape-selective catalysis will be interesting targets for the future. Specifically organized secondary and tertiary structures that are synthesized by using novel cations and polyanions may open up new areas of catalysis. If the structure, composition and stability of polyanions are properly controlled on supports, solid HPA catalysts will find much wider practical applications. The development of regeneration methods for deactivated HPA catalysts is another important subject for practical applications. As for catalysis in solution, unconventional reaction fields such as multi-phase catalysis are promising. From the viewpoint of fundamental study of HPA catalysis, the basicity of the surface of the heteropolyanion (or unique complexation character) together with its role in catalysis is of interest and understanding of the catalytic reaction at the molecular/atomic level is expected to be accomplished in the near future.

More progress is anticipated for oxidation catalysis of HPAs although oxidation catalysis lies outside the scope of the present article. The design of primary structures (structure and composition) has been successful for oxidation in solution and may be extended to heterogeneous catalysis, if HPAs are stabilized or reaction systems chosen carefully. Examples include diiron and dimanganese substsituted Keggin anions as shown in Fig. 1(c)[57] which efficiently catalyze selective oxidation of alkanes, although enhancement of reaction rate is still desirable. A variety of polyanion structures and compositions (new and known) as well as recent progress in novel synthetic methods promises the development of efficient catalysts based on HPAs. For example, an exotic HPA synthesized by Newmann and Dahan is efficient in selective oxidation.[58] Owing to various advantages, HPAs are hoped to play important roles as green catalysts in chemical syntheses in a sustainable manner.

Acknowledgements

Useful discussions with Profs. T. Okuhara, K. Inumaru, and N. Mizuno, Drs. G. Koyano and T. Ito, and Ms. S. Uchida are gratefully acknowledged. Thanks is given to Showa Denko Co. Ltd. for permitting the use of the photo of the Plant (cover).

Notes and references

1 J. M. Thomas, *Angew. Chem., Int. Ed.*, 1988, **27**, 1673.
2 M. Misono, *Stud. Surf. Sci. Catal.*, 1990, **54**, 13.
3 C. L. Hill, ed., *Chem. Rev.*, 1998, **98** (1).
4 See, for example: G. A. Tsigdinos, *Top. Curr. Chem.*, 1978, **76**, 1; M. T. Pope, *Heteropoly and Isopoly Oxometalates*, Springer-Verlag, Berlin, 1983.
5 See, for example: (*a*) M. Misono, *Catal. Rev.-Sci. Eng.*, 1987, **29**, 269; M. Misono, 1988, **30**, 339; (*b*) T. Okuhara, N. Mizuno and M. Misono, *Adv. Catal.*, 1996, **41**, 113; (*c*) N. Mizuno and M. Misono, *Chem. Rev.*, 1998, **98**, 199; (*d*) I. V. Kozhevnikov and K. I. Matveev, *Appl. Catal.*, 1983, **5**, 135; (*e*) I. V. Kozhevnikov, *Chem. Rev.*, 1998, **98**, 171; (*f*) Y. Izumi, K. Urabe and A. Onaka, *Zeolite, Clay, and Heteropoly acids in Organic Reactions*, Kodansha, Tokyo, VCH, Weinheim, 1992; (*g*) Y. Ono, in *Perspectives on Catalysis*, ed. J. M. Thomas and K. I. Zamaraev, Blackwell, London, 1992, p. 341; (*h*) A. Corma, *Chem. Rev.*, 1995, **95**, 559.
6 M. Misono and N. Nojiri, *Appl. Catal.*, 1990, **64**, 1; N. Nojiri and M. Misono, *Appl. Catal.*, 1993, **93**, 103.
7 M. Misono, K. Sakata, Y. Yoneda and W. Y. Lee, *Proc. 7th Int. Congr. Catal., Tokyo*, 1980, p. 1047.
8 M. Misono, *Proc. 10th Int. Congr. Catal., Budapest*, 1992, p. 69, Elsevier, Amsterdam/Akademiai Kiado, Budapest, 1993.
9 T. Komaya and M. Misono, *Chem. Lett.*, 1983, 1177; N. Mizuno, T. Watanabe and M. Misono, *J. Phys. Chem.*, 1990, **94**, 890.
10 T. Okuhara, A. Kasai, N. Hayakawa, Y. Yoneda and M. Misono, *J. Catal.*, 1983, **83**, 121.
11 S. Tatematsu, T. Hibi, T. Okuhara and M. Misono, *Chem. Lett.*, 1980, 865.
12 T. Okuhara, T. Nishimura, H. Watanabe, K. Na and M. Misono, in *Acid-Base Catalysis II*, Kodansha, Tokyo/Elsevier, Amsterdam, 1994, p 419.
13 M. Misono, N. Mizuno, H. Mori, K. Y. Lee and J. Jiao, *Stud. Surf. Sci. Catal.*, 1991, **67**, 87.
14 M. Misono, I. Ono, G. Koyano and A. Aoshima, *Pure Appl. Chem.*, 2000, **72**, 1305.
15 M. Misono, *C. R. Acad. Sci. Paris, Ser. IIc, Chim.*, 2000, **3**, 471.
16 (*a*) T. Kengaku, Y. Matsumoto, K. Na and M. Misono, *J. Mol. Catal.*, 1998, **134**, 237; (*b*) G. Koyano, K. Ueno and M. Misono, *Appl. Catal. A: Gen.*, 1999, **181**, 267.
17 Y. Toyoshi, T. Nakato and T. Okuhara, *Bull. Chem Soc. Jpn.*, 1998, **71**, 2817.
18 (*a*) S. Shikata and M. Misono, *Chem. Commun.*, 1998, 1293; (*b*) S. Shikata, T. Okuhara and M. Misono, *J. Mol. Catal. A: Chem.*, 1995, **100**, 49.
19 A. Malecka, J. Pozniczek, A. Micek-Ilnicka and A. Bielanski, *J. Mol. Catal. A: Chem.*, 1999, **138**, 67.
20 (*a*) T. Saito, G. Koyanao and M. Misono, *Chem. Lett.*, 1998, 1075; (*b*) G. Koyano, T. Saito, M. Hashimoto and M. Misono, *Stud. Surf. Sci. Catal.*, 2000, **130**, 3077.
21 C. Peze, S. Bordiga and A. Zecchina, *Langmuir*, 2000, **16**, 8139.
22 S. Uchida, K. Inumaru and M. Misono, *J. Phys. Chem. B*, 2000, **104**, 8108.
23 T. Okuhara, T. Nishimura and M. Misono, *Stud. Surf. Sci. Catal.*, 1996, **101**, 559.
24 R. S. Drago, J. A. Dias and T. O. Maier, *J. Am. Chem. Soc.*, 1997, **119**, 7702.
25 T. Okuhara, H. Watanabe, T. Nishimura, K. Inumaru and M. Misono, *Chem. Mater.*, 2000, **12**, 2230.
26 B. B. Bardin, S. V. Bordaweker, M. Neurock and R. J. Davis, *J. Phys. Chem. B*, 1998, **102**, 10817.
27 J. B. Moffat, *J. Mol. Catal.*, 1984, **26**, 385; H. Taketa, S. Katsuki, K. Eguchi, T. Seiyama and N. Yamazoe, *J. Phys. Chem.*, 1986, **90**, 2959.
28 T. T. Ali-Saad, A. A. El-Smahy, R. M. Gabr, R. V. Belosludov, S. Takami, M. Kubo, A. Miyamoto and M. Misono, *87th Symp. Catal. Soc. Jpn.*, April, 2001.
29 (*a*) T. Baba and Y. Ono, *Appl. Catal.*, 1999, **181**, 227; (*b*) T. Baba, Y. Hasada, M. Nomura, Y. Ohono and Y. Ono, *J. Mol. Catal.*, 1996, **114**, 247; (*c*) T. Baba, N. Komatsu, H. Sawada, Y. Yamada, T. Takahashi, H. Sugisawa and Y. Ono, *Langmuir*, 1999, **15**, 7894.
30 M. Guisnet, Ph. Bichon, N. S. Gnep and N. Essayem, *Top. Catal.*, 2000, **11/12**, 247.
31 T. Okuhara and T. Nakato, *Catal. Surv. Jpn.*, 1998, **2**, 31.
32 Y. Izumi, M. Ogawa and K. Urabe, *Appl. Catal.*, 1995, **132**, 127.
33 A. Parent and J. B. Moffat, *J. Catal.*, 1998, **177**, 335.
34 T. Ito, K. Inumaru and M. Misono, *Chem. Mater.*, 2001, **13**, 824.
35 T. Yamada, Y. Yoshinaga and T. Okuhara, *Bull. Chem. Soc. Jpn.*, 1998, **71**, 2727.
36 S. Berndt, D. Herein, F. Zemlin, E. Beckmann, G. Weinberg, J. Schutze, G. Metsl and R. Schlogl, *Ber. Bunsen-Ges. Phys. Chem.*, 1998, **102**, 763.
37 K. Inumaru, H. Nakajima, T. Ito and M. Misono, *Chem. Lett.*, 1996, 559; T. Oto, I. K. Song and M. Misono, *Chem. Lett.*, 1997, 727.
38 T. Ito, K. Inumaru and M. Misono, *J. Phys. Chem. B*, 1997, **101**, 9958.
39 T. Ito, K. Inumaru and M. Misono, *Chem. Lett.*, 2000, 830.
40 Y. Yoshinaga, K. Seki, T. Nakato and T. Okuhara, *Angew. Chem., Int. Ed. Engl.*, 1997, **36**, 2833; T. Okuhara, T. Yamada, K. Seki, K. Johkan and T. Nakato, *Microporous Mesoporous Mater.*, 1998, **21**, 637.
41 T. Okuhara, R. Watanabe and Y. Yoshinaga, *ACS Symp. Ser.*, 2000, **758**, 369.
42 N. Mizuno, K. Inumaru and M. Misono, *Hyoumen Kagakkaishi*, 1989, **10**, 21.
43 T. Yamada and T. Okuhara, *Langmuir*, 2000, **16**, 2321.
44 (*a*) T. Okuhara, M. Kimura and T. Nakato, *Chem. Lett.*, 1997, 839; (*b*) T. Nakato, M. Kimura, S. Nakata and T. Okuhara, *Langmuir*, 1998, **14**, 319.
45 T. Okuhara, X. Chen and H. Matsuda, *Appl. Catal. A: Gen.*, 2000, **200**, 109.

46 K. Sano, H. Uchida and S. Wakabayashi, *Catal. Surv. Jpn.*, 1999, **3**, 55.
47 K. Na, T. Okuhara and M. Misono, 1997, **170**, 96; K. Na, T. Okuhara and M. Misono, *J. Mol. Catal.*, 1997, **115**, 499; Y. Liu, G. Koyano and M. Misono, *Top. Catal.*, 2000, **11**/**12**, 239.
48 T. Suzuki and T. Okuhara, *Chem. Lett.*, 2000, 470; T. Sazuki and T. Okuhara, *Catal. Lett.*, in press.
49 M. R. H. Siddiqui, S. Holmes, H. He, W. Smith, E. N. Coker and I. V. Kozhevnikov, *Catal. Lett.*, 2000, **66**, 53.
50 Y. Izumi, M. Ono, M. Ogawa and K. Urabe, *Chem. Lett.*, 1993, 825; Y. Izumi, K. Hisano and T. Hida, *Appl. Catal. A: Gen.*, 1999, **181**, 277.
51 Y. Guo, Y. Wang, C. Hu, Y. Wang and E. Wang, *Chem. Mater.*, 2000, **12**, 3501.
52 S. Soled, S. Miseo, G. McVicker, W. E. Gates, A. Gutierrez and J. Paes, *Catal. Today*, 1997, **36**, 441.
53 (*a*) C. De. Castro, J. Primo and A. Corma, *J. Mol. Catal. A: Chem.*, 1998, **134**, 215; (*b*) I. V. Kozhevnikov, A. Sinnema, R. J. J. Jansen, K. Pamin and H. van Bekkum, *Catal. Lett.*, 1995, **30**, 241.
54 (*a*) Y. Watanabe, K. Yamamoto and T. Tatsumi, *J. Mol. Catal. A: Gen.*, 1999, **145**, 281; (*b*) T. Tatsumi, K. Yamamoto, H. Tajima and H. Tominaga, *Chem. Lett.*, 1992, 816.
55 B. Sulikowski, J. Haber, A. Kubacka, K. Pamin, Z. Olejniczak and J. Ptaszynski, *Catal. Lett.*, 1996, **39**, 27; S. Mukai, T. Masuda, I. Ogino and K. Hashimoto, *Appl. Catal. A: Gen.*, 1997, **165**, 219.
56 (*a*) W. Turek, E. S. Pormarzanska, A. Pron and J. Haber, *J. Catal.*, 2000, **189**, 297; (*b*) A. Bielanski, R. Dziembaj and A. Malecka, *J. Catal.*, 1999, **185**, 363; (*c*) S. L. Lim, Y. H. Kim, G. I. Park, W. Y. Lee, I. K. Song and H. K. Youn, *Catal. Lett.*, 1999, **60**, 199.
57 N. Mizuno, C. Nozaki, I. Kiyoto and M. Misono, *J. Am. Chem. Soc.*, 1998, **120**, 9267.
58 R. Neumann and M. Dahan, *Nature*, 1997, **388**, 353.
59 M. J. Verhoef, P. J. Kooyman, J. A. Peters and H. van Bekkum, *Microporous Mesoporous Mater.*, 1999, **27**, 365.
60 Y. Izumi, K. Hisano and T. Hida, *Appl. Catal A: Gen.*, 1999, **181**, 277.
61 T. Blasco, A. Corma, A. Martinez and P. Martinez-Escolano, *J. Catal.*, 1998, **177**, 306.
62 P. Y. Gayraud, I. H. Stewart, S. B. Deroune-Abd Hamid, N. Essayem, E. G. Derouane and J. C. Vedrine, *Catal. Today*, 2000, **63**, 223.
63 G. Meuzelaar, L. Maat, R. Sheldon and I. V. Kozhevnikov, *Catal. Lett.*, 1997, **45**, 249.
64 A. Corma, A. Martinez and C. Martinez, *J. Catal.*, 1996, **164**, 422; N. Essayem, S. Keiger, G. Coudurier and J. C. Vedrine, *Stud, Surf. Sci. Catal.*, 1996, **101**, 591; B. B. Bardin and R. Davis, *Top. Catal.*, 1998, **6**, 77; K. Na, T. Okuhara and M. Misono, *J. Catal.*, 1997, **170**, 96; Y. Liu, K. Na and M. Misono, *J. Mol. Catal. A: Chem.*, 1999, **141**, 145; Y. Liu, G. Koyano and M. Misono, *Top. Catal.*, 2000, **11**/**12**, 239; C. Travers, N. Essayem, M. Delage and S. Quelen, *Catal. Today*, 2000, **65**, 355.